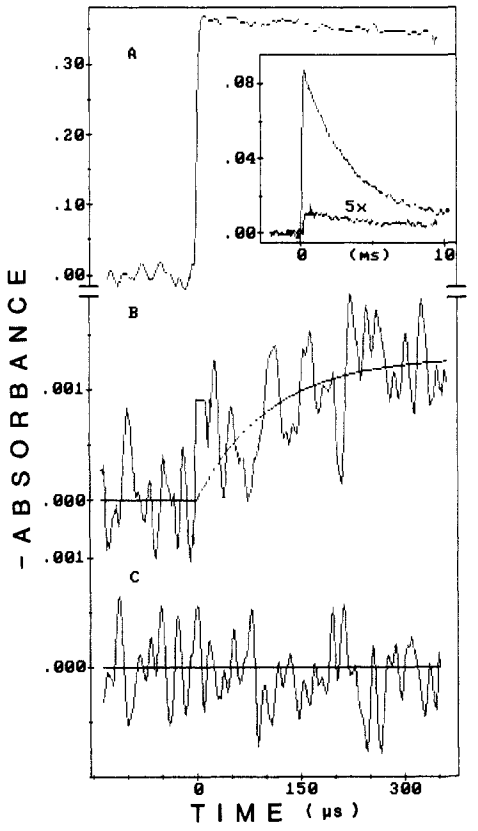

Figure 2. (A) Short-time absorbance change for ^{3}ZnP in [ZnC*c*P,-Fe^{III}C*c*(yeast-isozyme-2)], monitored at 434 nm. (Inset) Long-time decay of absorbance of ^{3}ZnP (low photolysis power) and of intermediate B (x5). (B) Growth of intermediate B, after photolysis of [ZnC*c*P,-Fe^{III}C*c*(yeast-isozyme-2)]; λ = 444.5 nm. Solid line is a fit to eq 3. Because of a signal from scattered light, five channels after t = 0 have been suppressed; these were not included in the fitting procedure. (C) Control: [ZnC*c*P,Fe^{II}C*c*] flashed under the same experimental condition as in (B). Conditions: 1.0 mM potassium phosphate buffer pH 7.0 at 25 °C. The signal in panel A represents the accumulation of 10 transients; the inset to (A) involved 1 transient for ^{3}ZnP and 16 for B; signals in (B) and (C) each represent 32 transients.

wavelength also is the maximum of the ^{3}ZnC*c*P/ZnC*c*P difference spectrum.

Flash excitation of the [ZnC*c*P,Fe^{III}C*c*(tuna)] complex gives a small but well-defined transient absorbance at 444.5 nm, whereas ZnC*c*P and [ZnC*c*P,Fe^{II}C*c*(tuna)] show a clean isosbestic point at 444.5 nm, and tuna Fe^{III}C*c* alone gives no observable transient. During the lifetime of the ^{3}ZnP, the transient absorbance grows with a rate constant equal to k_p (Figure 1, Inset), as predicted by eq 3 under the condition $k_b << k_p$. In this case B should persist after ^{3}ZnP has disappeared and decrease slowly, with rate constant k_b, precisely as seen in Figure 1. A fit to the long-time decay of the transient signal gives $k_b = 12 \pm 4$ s^{-1}. Because B persists, the transient also could be detected at long time after the complete decay of the ^{3}ZnP, using other wavelengths. The rate constant, k_b, is invariant with λ and the extrapolated zero-time absorbance change, $\Delta A'_0 = [\epsilon_B - \epsilon_A]A^*_0 k_t/(k_p - k_b)$ (eq 3), agrees in sign and magnitude with that expected from measured rate constants and static absorbance spectra.

A slow transient is not observed at any wavelength for the homologous complex[11] [ZnC*c*P, yeast Fe^{III}C*c*]. However, a rapid transient is detectable. At short times (Figure 2), the ^{3}ZnP signal, monitored at 434 nm, appears with the instrumental time constant and then remains essentially invariant. In contrast, at 444.5 nm a weak absorbance associated with intermediate B is seen to rise with a high, but finite, rate (Figure 2B) and then decay in parallel with ^{3}ZnP (inset, Figure 2A). As with the tuna C*c*, no signal is observed at 444.5 nm with the reference compounds Fe^{III}C*c*, ZnC*c*P, and [ZnC*c*P,Fe^{II}C*c*] (Figure 2C). This behavior is consistent with eq 3 in the limit $k_b >> k_p$, in which case k_b governs the increase of the absorbance of B at 444.5 nm; analysis gives $k_b = (1.1 \pm 0.5) \times 10^4$ s^{-1}.[11] As with tuna Fe^{III}C*c*, the sign and magnitude of the absorbance change in Figure 2B are consistent with the small amount of B predicted by the measured rates ($B(\tau)/A^*_0 \lesssim 10^{-2}$) and static absorbance spectra.

The large difference in rate constants for the thermal reaction (2) in complexes with two highly similar[12] C*c*, k_b(yeast)/k_b(tuna) $\sim 10^3$, is a striking display of influence of the protein on electron transfer in the physiological direction. This difference undoubtedly reflects different C*c*P–C*c* docking in the homologous complex, consistent with the higher affinity of C*c*P for yeast C*c* than for the horse or tuna proteins.[7e] If this charge-transfer process involves superexchange contributions[13] from intervening residues, as can be inferred from the modeling studies[8] and the evolutionary conservation of phenylalanine 82 of C*c*,[12] then it could be especially sensitive to subtle conformational alterations of the protein–protein interface.[14] In addition, application of the principle of microscopic reversibility to the protein dependence of the k_b/k_t ratio, $k_b/k_t \sim 0.5$ for tuna C*c*, but $k_b/k_t \sim 500$ for yeast C*c*, indicates a conformational rearrangement within the complex following the ^{3}ZnP → Fe^{III}P electron transfer.[15] This, of course, is as expected:[14] Solution[12] and X-ray diffraction structural studies[16] show that C*c* undergoes a conformational change upon reduction and changes in C*c*P also may occur. Clearly, a more precise understanding of the structures of the complexes between oxidized and reduced forms of C*c*P and of C*c* will be required in parallel with electron-transfer measurements.

Acknowledgment. This work has been supported by the National Institutes of Health, Grants HL 13531 (B.M.H.) and GM 19121 (E.M.).

(11) Results are similar for yeast iso-2 C*c*, yeast iso-1 C*c*, and yeast iso-1 C*c* that has been carboxymethylated at cysteine 103.

(12) Margoliash, E.; Schejter, A. *Adv. Protein Chem.* **1966**, *21*, 113.
(13) Miller, J. R.; Beitz, J. V. *J. Chem. Phys.* **1981**, *74*, 6750–6756.
(14) Rackovsky, S.; Goldstein, D. A. *Proc. Nat. Acad. Sci. U.S.A.* **1984**, *81*, 5901–5905.
(15) Analogous observations have been made earlier. Tabushi, I.; Yamamura, K.; Nishiya, T. *J. Am. Chem. Soc.* **1979**, *103*, 2785–2787.
(16) (a) Takano, T.; Richardson, R. E. *J. Mol. Biol.* **1981**, *153*, 79–94. (b) Takano, T.; Richardson, R. E. *J. Mol. Biol.* **1981**, *153*, 95–115.

Synthesis and Crystal and Molecular Structure of In(C_5Me_5): An Apparent Octahedral Cluster

O. T. Beachley, Jr.,* Melvyn Rowen Churchill, James C. Fettinger, J. C. Pazik, and L. Victoriano

Department of Chemistry
State University of New York at Buffalo
Buffalo, New York 14214

Received December 16, 1985

The synthesis and structural characterization of group 13 compounds can play an important role in the development of main-group organometallic chemistry. A topic of current interest centers on compounds with the metal in positive oxidation states which are less than 3. In group 13 chemistry the fully characterized compounds in the +1 oxidation state include In(C_5H_5)[1,2] and Tl(C_5H_5).[3] The indium(I) compound is most readily prepared from InCl and LiC_5H_5 in diethyl ether.[2] An X-ray structural

(1) Fischer, E. O.; Hofmann, H. P. *Angew. Chem.* **1957**, *69*, 639.
(2) Peppe, C.; Tuck, D. G.; Victoriano, L. J. *Chem. Soc., Dalton Trans.* **1981**, 2592.
(3) (a) Fischer, E. O. *Angew. Chem.* **1957**, *69*, 207. (b) Meister, H. *Angew. Chem.* **1957**, *69*, 533. (c) Cotton, F. A.; Reynolds, L. T. *J. Am. Chem. Soc.* **1958**, *80*, 269. (d) Tyler, J. K.; Cox, A. P.; Sheridan, J. *Nature (London)* **1959**, *183*, 1182.

0002-7863/86/1508-4666$01.50/0

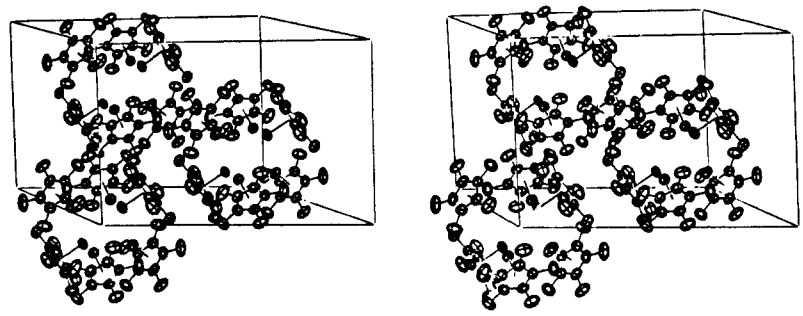

Figure 1. Stereoscopic view, showing the packing of the In(η^5-C_5Me_5) units into octahedral clusters (ORTEP II diagram, 30% probability ellipsoids for all non-hydrogen atoms).

study[4] reveals the presence of zig-zag polymeric chains of In(η^5-C_5H_5) units with very long In–"centroid" distances (3.19 Å). The distance between indium atoms which are arranged in apparent triangles is 3.99 Å. In contrast, the gas phase[5] consists of discrete monomeric In(η^5-C_5H_5) units with In–C distances (2.621 Å) which are significantly shorter than that observed for the solid state. In order to understand more fully the nature of organoindium(I) compounds, we report the synthesis and crystal and molecular structure of In(C_5Me_5). The new compound In(C_5Me_5) was prepared from InCl (4.92 mmol) and Li(C_5Me_5) (5.00 mmol) in diethyl ether. This combination of reagents leads to the formation of a deep yellow solution and heavy grey precipitate, indicative of a mixture of LiCl and indium metal. The yellow solution was separated from the solid in the reaction mixture by filtration. Removal of solvent and subsequent sublimation of the resulting yellow solid at 55 °C and 0.001 torr led to the isolation of In(C_5Me_5) as a yellow orange crystalline solid[7] (0.710 g, 2.84 mmol, 57.7% yield based on InCl). Crystals of crystallographic quality were grown by sublimation at 55 °C under high vacuum. The compound is *exceedingly* air- and moisture-sensitive. An initial product of hydrolysis is indium metal. Trace amounts of moisture convert the yellow orange crystals to a dark grey-green solid.

In(C_5Me_5) crystallizes in the rhombohedral space group $R\bar{3}$ (C_{3i}^2; No. 148) with unit cell parameters (hexagonal setting) a = 20.182 (4) Å, c = 13.436 (3) Å, V = 4739 (2) Å^3, and Z = 18. X-ray diffraction data (Mo Kα, 2θ = 4.5–50.0°) were collected on a Syntex $P2_1$ automated four-circle diffractometer by the coupled θ–2θ scan technique and were corrected for the effects of absorption (μ = 21.7 cm^{-1}). The structure was solved by Patterson and difference-Fourier methods and refined to R_F = 3.6% and R_{wF} = 3.3% for all 1870 unique data (R_F = 2.5% and R_{wF} = 2.9% for those 1444 reflections with $|F_o| > 6\sigma(|F_o|)$).

The packing of In(C_5Me_5) units within the unit cell is illustrated in Figure 1. They are arranged about centers of $\bar{3}$ (S_6) symmetry with indium atoms on the interior and η^5-C_5Me_5 units on the exterior of hexameric units. The In–In distances are all chemically equivalent, with values of 3.963 (1) Å around the C_3 axis and 3.943 (1) Å between atoms in the two triangular units; the molecule is thus based upon an octahedral In_6 core (see Figure 2). This In–In distance[4] is very similar to that observed in In(C_5H_5).

Individual In–C distances range from 2.581 (4) through 2.613 (4) Å, averaging 2.595 Å, and the In–"centroid" distance is 2.302 Å. Carbon–carbon distances within the carbocyclic ring are 1.397 (6)–1.417 (6) Å (average = 1.409 Å), while C(ring)–Me distances are 1.496 (10)–1.515 (9) Å (average = 1.508 Å). The C_5Me_5 skeleton has C_{5v} symmetry with all Me groups displaced from the ring and away from the indium atom by 0.092 (8)–0.110 (7) Å; the average deviation of 0.101 Å corresponds to a perpendicular angular displacement of 3.84°.

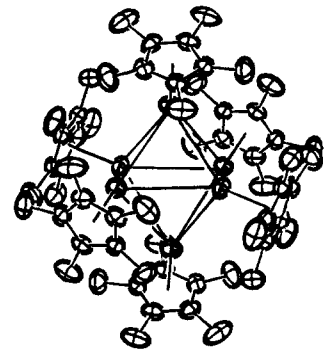

Figure 2. View of the hexameric octahedral cluster.

The volatility of In(C_5Me_5) suggests that the octahedral cluster has only marginal stability. Monomeric species are probably formed in the gas phase. However, some type of bonding interaction is required to counteract the repulsions between the ends of the dipole moments associated with bringing six monomeric (pentamethylcyclopentadienyl)indium units together in the solid state. Cyclopentadienylindium(I) has a significant experimental dipole moment[8] of 2.2 D, with the indium atom and its associated lone pair being the negative end of the molecule. It is also of interest that the structure of the hexaindium cluster $In_6(C_5Me_5)_6$ is significantly different from that observed for other stable main-group element clusters such as those for boron hydrides[9-11] and boron subhalides.[12,13] All boron-containing clusters have boron←hydrogen and boron←halogen vectors which point toward the centers of the clusters. The indium←centroid vectors do not point toward the center. The only fully characterized octahedral boron cluster[14] is $B_6H_6^{2-}$. The boron subhalide B_6Br_6 has been observed but the compound has not been fully characterized.[13] Similarly, $B_6[NMe_2AlMe_2]_6$ has been reported but no structural data are available.[15] Orbital and skeletal electron-counting conventions by Wade[9] and Williams[10] require each skeletal atom to provide one sp hybrid orbital and two p atomic orbitals for cluster bonding. Thus, the octahedral boron cluster, $B_6H_6^{2-}$, has seven pairs of skeletal bonding electrons whereas $In_6(C_5Me_5)_6$ has only six apparent electron pairs. The resulting disparities between the structural characteristics and the thermodynamic stabilities of these octahedral clusters could originate with the atomic orbitals which each skeletal atom provides for cluster bonding and/or with the number of available skeletal bonding electrons. Further details of the chemistry of (pentamethylcyclopentadienyl)- and related

(4) Frasson, E.; Menegus, F.; Panattoni, C. *Nature (London)* **1963**, *199*, 1087.
(5) Shibata, S.; Bartell, L. S.; Gavin, R. M., Jr. *J. Chem. Phys.* **1964**, *41*, 717.
(6) Lithium pentamethylcyclopentadienide was prepared from *n*-butyl lithium and pentamethylcyclopentadiene as a colorless solid.
(7) Anal. Calcd ($InC_{10}H_{15}$): C 48.03; H, 6.06. Found: C, 47.74; H, 6.04.
(8) Lin, C. S.; Tuck, D. G. *Can. J. Chem.* **1982**, *60*, 699.
(9) Wade, K. *Adv. Inorg. Radiochem.* **1976**, *18*, 1 and references therein.
(10) Williams, R. E. *Adv. Inorg. Radiochem.* **1976**, *18*, 67 and references therein.
(11) Rudolph, R. W. *Acc. Chem. Res.* **1976**, *9*, 446.
(12) Massey, A. G. *Chem. Br.* **1980**, *15*, 588. Saulys, D.; Morrison, J. A. *Inorg. Chem.* **1980**, *19*, 3057. Davan, T.; Morrison, J. A. *J. Chem. Soc., Chem. Commun.* **1981**, 250. Emery, S. L.; Morrison, J. A. *J. Am. Chem. Soc.* **1982**, *104*, 6790.
(13) Kutz, N. A.; Morrison, J. A. *Inorg. Chem.* **1980**, *19*, 3295.
(14) Schaeffer, R.; Johnson, Q.; Smith, G. S. *Inorg. Chem.* **1965**, *4*, 917.
(15) Amero, B. A.; Schram, E. P. *Inorg. Chem.* **1976**, *15*, 2842.

cyclopentadienylindium(I) derivatives will be reported in the near future.

Acknowledgment. This work was supported in part by the Office of Naval Research (O.T.B.).

Supplementary Material Available: Tables of atomic coordinates, thermal parameters, bond lengths, and bond angles (13 pages). Ordering information is given on any current masthead page.

Nonplanar, 6π-Electron Metallacyclic Alkylidene Complexes from Coupling of Coordinated Alkynes and η²-Iminoacyls on a Tantalum Center

M. David Curtis* and Julio Real

Department of Chemistry, The University of Michigan Ann Arbor, Michigan 48109

Received March 12, 1986

Certain complexes of niobium and tantalum are known to catalyze the polymerization and oligomerization of alkynes, but the details of the mechanism are obscure.[1] We here report the synthesis and transformations of certain alkyne–alkyl complexes of Ta which have bearing on alkyne polymerization catalysis and which lead to an increased understanding of the electronic factors which govern metallacyclic structures.

Treatment of CpTa(ArC≡CAr)Cl_2[2] with 2 equiv of MeLi gives essentially quantitative yields of CpTa (ArC≡CAr)Me_2 (**1**) (Ar = phenyl or *p*-tolyl). The Ta-Me carbons appear at δ 46.3 (q,

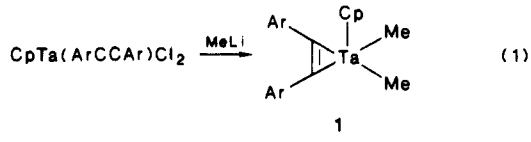

(1)

1

$^1J_{CH}$ = 120 Hz) and the coordinated acetylenic carbons at δ 239.4. The latter resonance is indicative of 4e⁻ donor acetylenes;[3] therefore, compound **1** is formally a 16-electron complex. Yellow **1** is stable for weeks in the absence of air.

Reaction of **1** with *t*-BuNC gave a nearly quantitative yield of the η²-iminoacyl complex **2** (eq 2).

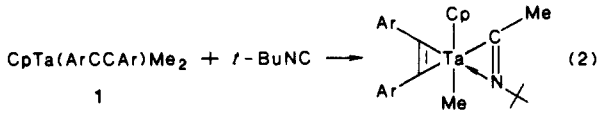

(2)

2

The structure of **2** has been determined crystallographically and the metrical parameters[4] are consonant with a description of the bonding as shown in eq 2. The overall structure is very similar to that of CpMo(RCCR)$_2$L complexes.[5] The ^{13}C NMR resonance of the iminoacyl carbon occurs at δ 241.1 and the alkyne carbon resonance appears as a single peak at δ 199.7 down to −80 °C. EHMO calculations also suggest a low barrier for end over end rotation of the coordinated alkyne.[6]

Heating a toluene solution of **2** causes the coordinated alkyne and η²-iminoacyl to couple and the five-membered metallacycle **3** forms quantitatively after 15 h at 90 °C.

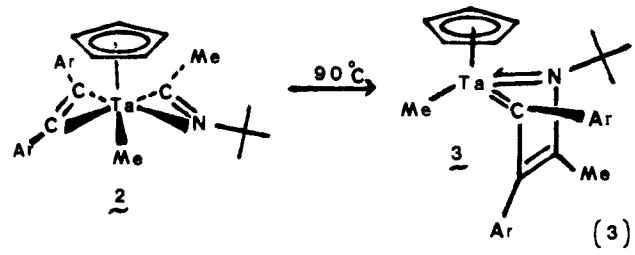

(3)

The structure of **3** is quite interesting. The TaC_3N ring is folded 120° (Figure 1) and the Ta—C_α and Ta—N distances in the metallacycle are both 1.98 (1) Å and are commensurate with Ta=C and Ta=N double bonds.[7,8] The C_α—C_β (1.48 (1) Å) and N—C'_β (1.40 (1) Å) bonds are relatively long, while the C_β–C'_β (1.39 (2) Å) distance is short. These distances suggest that the ring structure in **3** is a derivative of a metallacyclopenta*tri*ene (C, see below). This view is supported also by the ^{13}C NMR spectrum of **3**. The resonance of C_α occurs at δ 231.6 in the range expected for terminal alkylidenes, and the C_β and C'_β resonances are found at δ 95.7 and 121.5.

Thorn and Hoffmann have analyzed the electronic structure of d^0, d^6, and d^8 MC_4R_4 metallacyclopentadienes, A, and have described the requirements necessary to attain a delocalized or "aromatic" metallacycle, B.[9] Briefly, these requirements are that (1) the metal fragment possess an empty orbital to accept electrons from the π_2 MO of the C_4R_4 fragment and (2) a filled orbital to donate electrons to the empty π^*_3 MO (see below). The net

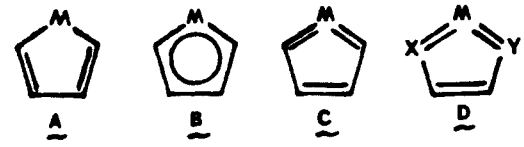

A **B** **C** **D**

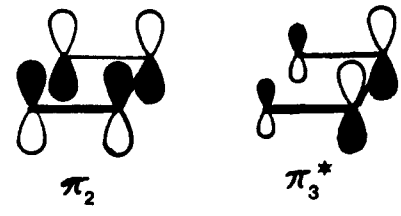

electron transfer from π_2 to π^*_3 decreases the C_α–C_β bond order and increases the C_β–C'_β bond order. At some point, these bond orders become equal and the "delocalized" structure B results. This synergic bonding interaction also results in M=C_α multiple bond character.

The cyclopenta*tri*ene structure C is then seen as an extreme case of the electron redistribution between π_2 and π^*_3 described above. EHMO calculations [10] show that the d^2, $CpNb(R)^+$ fragment has the requisite donor and acceptor orbitals and, of course, the $C_3NR_4^{1-}$ fragment is isoelectronic and isolobal with the $C_4R_4^{2-}$ fragments discussed by Thorn and Hoffman.[9]

The electronic driving force for the ring folding observed in **3** has been analyzed with the EHMO method.[10] The largest effect seems to be the relief of M···C_β *anti*bonding interactions when the ring is folded. In the bent configuration, the M–C_β overlap population is essentially zero but is −0.12 in the planar configuration. Other examples of bent, 6π-electron metallacycles are

(1) (a) Masuda, T.; Niki, A.; Isobe, E.; Higashimura, T. *Macromolecules* **1985**, *18*, 2109. (b) Masuda, T.; Isobe, E.; Higashimura, T. *J. Am. Chem. Soc.* **1983**, *105*, 7473. (c) Masuda, T.; Takahashi, T.; Higashimura, T. *J. Chem. Soc., Chem. Commun.* **1982**, 1297. (d) Cotton, F. A.; Hall, W. T.; Cann, K. J.; Karol, F. J. *Macromolecules* **1981**, *14*, 233.

(2) Curtis, M. D.; Real, J. *Organometallics* **1985**, *4*, 940.

(3) Templeton, J. L.; Ward, B. C. *J. Am. Chem. Soc.* **1980**, *102*, 3288.

(4) Some relevant distances: C=C, 1.30 (1); C=N, 1.25 (1); Ta—C-(iminoacyl), 2.10 (1); Ta—N, 2.12 (1); Ta—Me, 2.26 (1) Å. Complete tables of bond distances etc. are included in the supplementary material.

(5) Mead, K. A.; Morgan, H.; Woodward, P. *J. Chem. Soc., Dalton Trans.* *1983*, 271.

(6) EHMO calculations were performed on the Nb analogues. For related calculations, see: (a) Kreissel, F. R.; Sieber, W. J.; Hofmann, P.; Riedle, J.; Wolfgruber, M. *Organometallics* **1985**, *4*, 788. (b) Schilling, B. E. R.; Hoffmann, R.; Faller, J. W. *J. Am. Chem. Soc.* **1979**, *101*, 592.

(7) Ta=C distances range from 1.89 (3) to 2.07 (1) Å (av = 2.00 [8] Å): (a) Schrock, R. R.; Messerle, L. W.; Wood, C. D.; Guggenberger, L. J. *J. Am. Chem. Soc.* **1978**, *100*, 3793. (b) Guggenberger, L. J.; Schrock, R. R. *Ibid.* **1975**, *97*, 6578. (c) Churchill, M. R.; Hollander, F. J.; Schrock, R. R. *Ibid.* **1978**, *100*, 647. (d) Chamberlain, L.; Rothwell, I. P.; Huffman, J. C. *Ibid.* **1982**, *104*, 7338.

(8) Chisholm, M. H.; Huffman, J. C.; Tan, L.-S. *Inorg. Chem.* **1981**, *20*, 1859.

(9) Thorn, D. L.; Hoffmann, R. *Nouv. J. Chim.* **1979**, *3*, 39.

(10) Curtis, M. D., unpublished results.

0002-7863/86/1508-4668$01.50/0